

# The Role of Single Qubit Decoherence Time in Adiabatic Quantum Computation

M. H. S. Amin,<sup>1</sup> C. J. S. Truncik,<sup>1</sup> and D. V. Averin<sup>2</sup>

<sup>1</sup>*D-Wave Systems Inc., 100-4401 Still Creek Drive, Burnaby, B.C., V5C 6G9, Canada*

<sup>2</sup>*Department of Physics and Astronomy, SUNY Stony Brook, Stony Brook NY, USA*

We numerically study the evolution of an adiabatic quantum computer in the presence of a Markovian ohmic environment. We consider Ising spin glass systems with up to 20 coupled qubits that are independently coupled to the environment via two conjugate degrees of freedom. We demonstrate that the required computation time in the presence of the environment is of the same order as that for an isolated system, and is not limited by the single qubit decoherence time  $T_2^*$ , even when the minimum gap is much smaller than temperature. We also show that the behavior of the system can be efficiently described by a two-state model with only longitudinal coupling to the environment.

Adiabatic quantum computation [1] (AQC) is an attractive model of quantum computation (QC) as it naturally possesses some degree of fault tolerance. In AQC, a system starts from a readily accessible ground state of an initial Hamiltonian  $H_i$  and slowly evolves into the ground state of a final Hamiltonian  $H_f$  which encodes a solution to the problem of interest:

$$H_S(t) = [1 - s(t)]H_i + s(t)H_f, \quad (1)$$

where  $s(t) \in [0, 1]$  is a monotonic function of time  $t$ . Here, we only consider linear interpolation for which  $s(t) = t/t_f$ , where  $t_f$  is the total evolution time. Transitions out of the ground state can be caused by a Landau-Zener process [2] at the anticrossing ( $s=s^*$ ) where the gap  $g$  between the ground state  $|0\rangle$  and first excited state  $|1\rangle$  goes through a minimum:  $g_m \equiv g(s^*)$ . The probability of being in the ground state at the end of the adiabatic evolution is approximately ( $\hbar = k_B = 1$ )

$$P_{0f} = 1 - e^{-t_f/t_a}, \quad t_a \equiv \frac{4}{\pi g_m^2} \left| \langle 1 | \frac{dH_S}{ds} | 0 \rangle \right|_{s=s^*}, \quad (2)$$

To ensure a large  $P_{0f}$  one needs  $t_f \gtrsim t_a$ . The computation time is hence determined by  $t_a$  and thus by  $g_m$ .

In gate model QC there is no direct correspondence between the wavefunction and the instantaneous system Hamiltonian. The Hamiltonian is only applied at the time of gate operations and usually affects only a few qubits. The wavefunction, therefore, is strongly affected by the environment and is irreversibly altered after the decoherence time, which is typically of the order of the single qubit dephasing time  $T_2^*$ . Thus decoherence imposes an upper limit on the total computation time, unless quantum error correction schemes (which require significant resources) are utilized. This is not true for AQC as the wavefunction is always very close to the instantaneous ground state of the system Hamiltonian and is consequently more stable against decoherence. Intuitively, one expects decoherence to drive the density matrix towards being diagonal in the energy basis, which is not harmful for AQC but is detrimental for gate model QC. Despite several papers that have demonstrated such robustness [4, 5, 6, 7, 8, 9], this issue is still a subject

of debate. Much of the criticism stems from the fact that previous AQC studies have either used a two-state model to describe the behavior of a multi-level system at the anticrossing, or assumed noise models that are not motivated by physical implementations. In this paper, we numerically study the quantum evolution of a multi-qubit system with a quite general and realistic coupling to the environment.

Consider a very general Hamiltonian  $H(t) = H_S(t) + H_B + H_{\text{int}}$ , which includes system, bath, and interaction terms, respectively. The dynamics of the total (system + environment) density matrix are governed by the Liouville equation [10]:  $\dot{\rho}(t) = -i[H(t), \rho(t)]$ . The reduced density matrix for the system is obtained by partially tracing over the environmental degrees of freedom:  $\rho_S = \text{Tr}_B[\rho]$ . Let  $|n(t)\rangle$  denote the instantaneous eigenstates of the system Hamiltonian:  $H_S(t)|n(t)\rangle = E_n(t)|n(t)\rangle$ . In such a basis, we define  $\rho_{nm}(t) = \langle n(t) | \rho_S(t) | m(t) \rangle$ . Taking the time derivative, we obtain (dropping explicit time dependences)

$$\dot{\rho}_{nm} = \langle n | \dot{\rho}_S | m \rangle + \langle \dot{n} | \rho_S | m \rangle + \langle n | \rho_S | \dot{m} \rangle. \quad (3)$$

Let us begin by focusing on the first term in (3), which is responsible for the decay processes. We treat this term quasi-statically, which means we assume that the evolution of the Hamiltonian is much slower than the environmentally induced decay rates so that we can treat the eigenstates as time independent. We work in the interaction picture in which the density matrix,  $\rho_I(t) = U^\dagger(t)\rho(t)U(t)$ , evolves according to  $\dot{\rho}_I(t) = -i[H_I(t), \rho_I(t)]$ , with  $U(t) = e^{-i \int_0^t (H_S + H_B) d\tau}$  and  $H_I(t) = U^\dagger(t)H_{\text{int}}(t)U(t)$ . Integrating the above differential equation, we obtain  $\rho_I(t) = \rho_I(0) - i \int_0^t d\tau [H_I(\tau), \rho_I(\tau)]$ . After one iteration and taking derivatives with respect to  $t$ , we find

$$\dot{\rho}_I(t) = -i[H_I(t), \rho_I(0)] - \int_0^t d\tau [H_I(t), [H_I(\tau), \rho_I(\tau)]]. \quad (4)$$

We now introduce a few simplifying approximations. First, we assume that the effect of the system on the environment is so small that the bath's density matrix in

the right hand side of (4) can be represented by  $\rho_B(0)$  at all times and that the total density matrix can be written as a direct product:  $\rho_I(t) = \rho_{SI}(t)\rho_B(0)$ . We also assume that the bath has a correlation time  $\tau_B$  shorter than all decay times so that we can use the Markovian approximation to replace  $\rho_{SI}(\tau)$  with  $\rho_{SI}(t)$  inside the integral. Tracing over the bath's degrees of freedom and assuming that the first-order term in  $H_I$  vanishes after averaging, we find

$$\dot{\rho}_{SI}(t) = - \int_0^t d\tau \text{Tr}_B[H_I(t), [H_I(\tau), \rho_{SI}(t)\rho_B(0)]] . \quad (5)$$

After some manipulation, the first term in (3) becomes

$$\begin{aligned} \langle n|\dot{\rho}_S|m\rangle &= -i\omega_{nm}\rho_{nm} + e^{-i\omega_{nm}t}\langle n|\dot{\rho}_{SI}|m\rangle \\ &= -i\omega_{nm}\rho_{nm} - R_{nmkl}\rho_{kl}, \end{aligned} \quad (6)$$

where  $\omega_{nm} = E_n - E_m$ ,

$$\begin{aligned} R_{nmkl} &= \delta_{lm}\Gamma_{nrrk}^{(+)} + \delta_{nk}\Gamma_{lrrm}^{(-)} - \Gamma_{lmnk}^{(+)} - \Gamma_{lmnk}^{(-)}, \\ \Gamma_{lmnk}^{(+)} &= \int_0^\infty dt e^{-i\omega_{nk}t}\langle \tilde{H}_{I,lm}(t)\tilde{H}_{I,nk}(0)\rangle, \\ \Gamma_{lmnk}^{(-)} &= \int_0^\infty dt e^{-i\omega_{lm}t}\langle \tilde{H}_{I,lm}(0)\tilde{H}_{I,nk}(t)\rangle, \\ \tilde{H}_{I,nm}(t) &= \langle n|e^{iH_B t}H_{\text{int}}(t)e^{-iH_B t}|m\rangle. \end{aligned} \quad (7)$$

Here,  $\langle \dots \rangle \equiv \text{Tr}_B[\rho_B \dots]$ , and summation over repeated indices is implicit. Substituting (6) into (3), we obtain

$$\dot{\rho}_{nm} = -i\omega_{nm}\rho_{nm} - (R_{nmkl} - M_{nmkl})\rho_{kl}, \quad (8)$$

where  $M_{nmkl} = \delta_{nk}\langle l|\dot{n}\rangle + \delta_{ml}\langle \dot{n}|k\rangle$ . The tensors  $M_{nmkl}$  and  $R_{nmkl}$  are responsible for non-adiabatic and thermal transitions, respectively. For a time independent Hamiltonian,  $M_{nmkl} = 0$  and (8) becomes the Bloch-Redfield equations [10, 11].

The state derivatives,  $|\dot{n}\rangle$  etc., can be calculated numerically. It is important to ensure that the equation stays trace preserving, which requires  $\text{Re}\sum_{n,m}\langle n|\dot{n}\rangle = 0$ . This condition is *exactly* satisfied (even with the truncation discussed below), if we write  $\langle n(t)|\dot{n}(t)\rangle = \frac{1}{4\delta t}\{\langle n(t+\delta t)| + \langle n(t-\delta t)|\}\{\dot{m}(t+\delta t) - \dot{m}(t-\delta t)\}$ .

We consider a quite general interaction Hamiltonian

$$H_{\text{int}} = - \sum_{i=1}^n \left( Q_x^{(i)}\sigma_x^{(i)} + Q_z^{(i)}\sigma_z^{(i)} \right), \quad (9)$$

where  $Q_\alpha^{(i)}$  are heat bath operators. Using (7), and assuming uncorrelated heat baths, we find

$$\begin{aligned} \Gamma_{lmnk}^{(+)} &= \frac{1}{2} \sum_{i,\alpha} S_\alpha^{(i)}(-\omega_{nk})\sigma_{\alpha,lm}^{(i)}\sigma_{\alpha,nk}^{(i)}, \\ \Gamma_{lmnk}^{(-)} &= \frac{1}{2} \sum_{i,\alpha} S_\alpha^{(i)}(\omega_{lm})\sigma_{\alpha,lm}^{(i)}\sigma_{\alpha,nk}^{(i)}, \end{aligned} \quad (10)$$

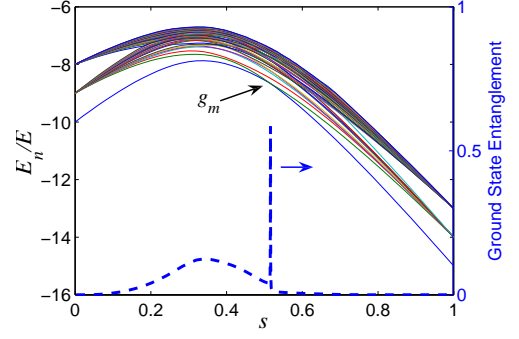


FIG. 1: Energy spectrum for a 20 qubit instance with minimum gap  $g_m/E \approx 5 \times 10^{-4}$ . Only the first 50 energy levels among a total  $\sim 10^6$  are shown. The dashed line represents ground state entanglement using (13).

where  $S_\alpha^{(i)}(\omega) = \int_{-\infty}^\infty dt e^{i\omega t}\langle Q_\alpha^{(i)}(t)Q_\alpha^{(i)}(0)\rangle$  are the bath spectral densities and  $\sigma_{\alpha,lm}^{(i)} = \langle l|\sigma_\alpha^{(i)}|m\rangle$ . Here, we have neglected the imaginary parts of  $\Gamma_{lmnk}^{(\pm)}$ , as they only shift the oscillation frequencies which can be adequately addressed via proper renormalization.

To model the spectral densities, we assume ohmic bosonic heat baths in thermal equilibrium [12]:  $S_\alpha^{(i)}(\omega) = \eta_\alpha^{(i)}\omega e^{-\omega/\omega_c}/(1 - e^{-\omega/T})$ . The dimensionless coefficients  $\eta_\alpha^{(i)}$  describe the strength of couplings between qubits and the environment and  $\omega_c$  is a cutoff frequency which we assume to be larger than all relevant energy scales. The Markovian approximation is valid as long as  $\tau_B \sim 1/\omega_c$  is shorter than all the decay times and the variation of the Hamiltonian is slow.

We now use the above model to study the evolution of a multi-qubit Ising system with initial and final Hamiltonians given by

$$\frac{H_i}{E} = -\frac{1}{2} \sum_i \Delta_i \sigma_x^{(i)}, \quad (11)$$

$$\frac{H_f}{E} = -\frac{1}{2} \sum_i h_i \sigma_z^{(i)} + \frac{1}{2} \sum_{i>j} J_{ij} \sigma_z^{(i)} \sigma_z^{(j)}, \quad (12)$$

where  $\sigma_{x,z}^{(i)}$  are the Pauli matrices corresponding to the  $i$ -th qubit,  $E$  is an energy scale, and  $\Delta_i$ ,  $h_i$ , and  $J_{ij}$  are dimensionless parameters. We consider square lattice configurations with nearest and next-nearest neighbor coupling between the qubits. We generate spin glass instances involving 6, 9, 12, 16, and 20 qubits by randomly choosing  $h_i$  and  $J_{ij}$  from  $\{-1, 0, 1\}$  and identifying small gap instances with non-degenerate final ground state (see, e.g., Fig. 1). Such instances are very rare and represent difficult problems; a degenerate ground state (multiple solutions) ensures higher probability of finding one of the solutions. We also choose  $\Delta_i = 1$  for all  $i$ .

Figure 1 shows the energy spectrum for a typical 20 qubit instance with a small  $g_m$ . The first two energy levels anticross near the middle of the evolution. In the same

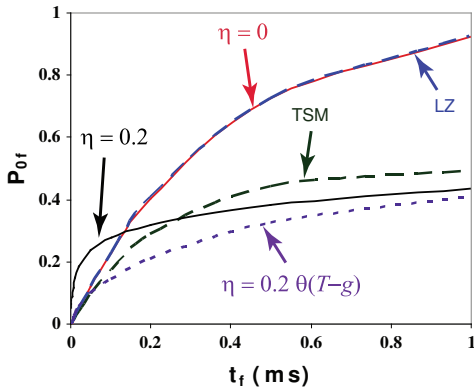


FIG. 2: Probability of success  $P_{0f}$  as a function of  $t_f$  for the 20 qubit instance of Fig. 1. The solid lines are calculated with ( $\eta = 0.2$ ) and without ( $\eta = 0$ ) coupling to the environment. Other parameters are  $E = 10$  GHz,  $T = 25$  mK. The dashed lines are obtained using analytical formulas (2) and (15). The dotted line is numerical calculation with  $\eta = 0.2 \theta(T - g)$ .

figure, we have also displayed the ground state entanglement calculated using a measure originally proposed by Meyer and Wallach [13]:

$$Q(|\psi\rangle) = \frac{1}{n} \sum_{k=1}^n 2(1 - \text{Tr}[\rho_k^2]) \quad (13)$$

where  $\rho_k \equiv \text{Tr}_{j \neq k} |\psi\rangle\langle\psi|$  is obtained by partially tracing over all qubits except the  $k$ -th one. The qubits become entangled during the evolution with a maximum entanglement at the anticrossing. However, the above measure is inadequate to describe the entanglement at the anticrossing as it does not account for thermal mixing. Unfortunately, no practical mixed state entanglement measure exists for more than two qubits [14].

To study the evolution as a function of time, we numerically integrate (8) starting from  $\rho_S(0) = |0\rangle\langle 0|$ . For a large number of qubits the computation becomes extremely time consuming because of the large number of matrix elements in  $\rho_S$ . However, since  $\rho_S$  is written in the energy basis at all times, it is possible to significantly simplify the computation by truncating  $\rho_S$  to only the lowest few energy levels that will be occupied during the evolution. To ensure small error, we increase the number of levels kept in our calculations until the result does not change. Typically a maximum of 7-8 energy levels are sufficient for the type of evolution and instances we consider here. For very slow evolution, even two states suffice to achieve acceptable accuracy. The numerical integration time can also be significantly reduced by refining the integration steps based on the gap size.

Figure 2 shows the probability of staying in the ground state at the end of the evolution as a function of  $t_f$  for the 20 qubit instance depicted in Fig. 1. For simplicity, we

have chosen the same coupling to the environment for all qubits:  $\eta_\alpha^{(i)} = \eta$ . Notice that with the chosen parameters  $g_m/T \sim 10^{-2}$ . As expected, the probability increases with  $t_f$ . For a closed system ( $\eta = 0$ ) the numerics agree with Eq. (2). For an open system ( $\eta = 0.2$ ), the probability is enhanced (compared to closed system) at small  $t_f$ . Such a thermally assisted behavior is the result of large relaxation after the anticrossing region and is not expected to enhance the scaling of the computation [7]. To confirm this, we have repeated the numerical calculations, but now allowing transitions only in the thermal mixing region [ $\eta = 0.2 \theta(T - g)$ ], i.e., eliminating the relaxation back to the ground state after the anticrossing. The result (dotted line in Fig. 2) shows no enhancement compared to the closed system. The increase of the probability at longer  $t_f$  is much slower for the open system. The important point is that the time scale for the probabilities to reach some non-vanishing value is almost the same [ $O(1$  ms)] for all curves. This was a generic property for all instances that we have studied regardless of the size of the gap [15].

We now compare the numerically calculated computation time with single qubit decoherence times. If the qubits are uncoupled ( $J_{ij}=0$ ), then the single qubit decoherence rates, in weak coupling limit, are given by  $1/T_2^* \sim S_\alpha^{(i)}(0) = O(\eta T)$ . For the parameters of Fig. 2,  $T_2^* \sim 10$  ns which is typical for superconducting qubits. This decoherence time is five orders of magnitude smaller than the computation time ( $\sim 1$  ms) for the problem of Fig. 2. Therefore, unlike the gate model QC, *in AQC the computation time is not limited by the single qubit decoherence time*. It should be noted that the qubits will go through an entangled state during the evolution, as demonstrated in Fig. 1, and such an entanglement will not be destroyed by the environment (except maybe at the anticrossing) as long as the system dominantly populates the ground state. Once again, this is in contrast to what is expected in gate model QC.

The numerical method presented here is valid only for a Markovian environment. Most environments, however, especially in superconducting systems, are not Markovian and have a significant amount of low frequency noise. In Ref. [9], we used a two-state model (TSM) to study the effect of a non-Markovian environment on AQC. For the rest of this paper, we focus on showing why a TSM is adequate for describing the performance of AQC in the small gap limit.

In order for the environment to be able to cause a transition out of the ground state, the interaction Hamiltonian should have nonzero matrix elements between the ground state and the target state. We introduce  $M_\alpha = (\frac{1}{n} \sum_i |\sigma_{\alpha,10}^{(i)}|^2)^{1/2}$ , which give the r.m.s. values of the matrix elements of Pauli matrices  $\sigma_\alpha^{(i)}$  between the lowest two states. They represent some average behavior of the corresponding matrix elements. Moreover,

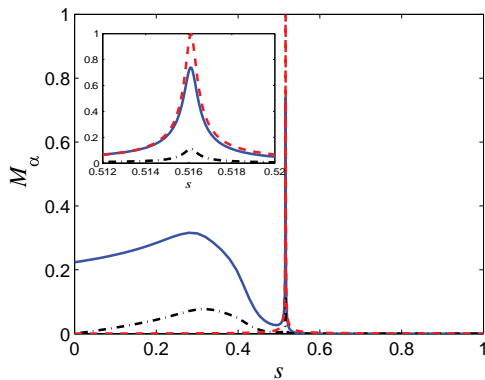


FIG. 3: (a) Matrix elements as a function of  $s$ . Solid (blue) line is  $M_z$ , dashed-dotted (black) line is  $M_x$  and the dashed (red) line is  $M_z^{\text{TSM}}$  obtained from a two state model keeping only the longitudinal coupling to the environment. The inset shows the same curves zoomed near the anticrossing.

if all qubits have the same coupling  $\eta$  to the environment, then the relaxation rate between the two states is given by  $\gamma = n(M_x^2 + M_z^2)\tilde{S}(\omega_{10})$ , where  $\tilde{S}(\omega)$  is the symmetrized spectral density of the (uncorrelated) baths. Figure 3(a) displays  $M_x$  and  $M_z$  as a function of  $s$  for the system of Fig. 1. Except for the initial region, they both show the same behavior: a sharp peak at the anticrossing, with a width proportional to  $g_m$ , followed by a vanishingly small value. For small  $T$  the excitation from the ground state will be suppressed everywhere except near the anticrossing where  $g < T$ .

The transitions at the anticrossing can be efficiently described by an effective two-state Hamiltonian:

$$\begin{aligned} H_S^{\text{TSM}} &= -\frac{1}{2}(g_m\tau_x + \epsilon\tau_z), \\ H_{\text{int}}^{\text{TSM}} &= -(Q_x^{\text{TSM}}\tau_x + Q_z^{\text{TSM}}\tau_z), \end{aligned} \quad (14)$$

where  $\tau_\alpha$  are the Pauli matrices in the two-state subspace,  $\epsilon = 2\tilde{E}(s - s^*)$ , with  $s^*$  being the position of the anticrossing and  $\tilde{E}$  an energy scale (close to  $E$  in our case) characterizing the anticrossing. Let us introduce matrix elements  $M_x^{\text{TSM}} = |\langle 0|\tau_x|1\rangle| = |\cos\theta|$  and  $M_z^{\text{TSM}} = |\langle 0|\tau_z|1\rangle| = |\sin\theta|$ , which are responsible for the transitions between the two levels, where  $\tan\theta = g_{\text{min}}/\epsilon$ . It is clear that  $M_x^{\text{TSM}}$  has a dip, instead of a peak, at the anticrossing, hence is completely different from the  $M_{x,z}$  above. On the other hand, except for an overall factor,  $M_z^{\text{TSM}}$  has the same shape as both  $M_{x,z}$  (see the inset of Fig. 3). Thus, in order for the effective two-state model to give the same result as the full system, it only needs to couple to the environment via  $\tau_z$  (i.e.,  $Q_x^{\text{TSM}} = 0$ ). For large transverse coupling to the environment, one would not expect an agreement with TSM because of the significant relaxation away from the anticrossing caused by such coupling. From the TSM Hamiltonian with longitudinal coupling, success probability in the large- $T$  limit, for an ohmic or subohmic environment, is found as [7, 9]

$$P_{0f}^{\text{TSM}} = \frac{1}{2}(1 - e^{-2t_f/t_a}), \quad (15)$$

This formula is also plotted in Fig. 2. The qualitative agreement with other curves on the figure indicates that most of the transition occur in small gap regions ( $g \ll T$ ) and TSM is adequate to describe such processes.

To summarize, by studying spin glass instances of up to 20 qubits (only one is illustrated), we have explicitly demonstrated that the computation time in AQC can be much longer than single qubit decoherence time  $T_2^*$ . We have also shown that a two-state model with longitudinal coupling to the environment can efficiently describe the physics of transitions at the anticrossing. Using such a model, the computation time scale was shown to be unaffected by an ohmic environment, in agreement with the numerical results. This effect was not due to suppression of transitions by a gap, as the minimum gap in the instances we have chosen was much smaller than temperature and decoherence strength. It should be emphasized that the above results were obtained under the assumption of weak coupling to the environment, for which the discrete energy structure of  $H_S$  is approximately preserved (except for some renormalization). For strong coupling to the environment, the interaction Hamiltonian will dominate and the above method will not hold.

The authors are grateful to A.J. Berkley, P. Bunyk, V. Choi, R. Harris, J. Johansson, M.W. Johnson, S. Lloyd, and G. Rose for useful discussions.

- 
- [1] E. Farhi, J. Goldstone, S. Gutmann, J. Lapan, A. Lundgren, and D. Preda, *Science* **292**, 472 (2001).
  - [2] L.D. Landau, *Phys. Z. Sowjetunion* **2**, 46 (1932); C. Zener, *Proc. R. Soc. A* **137**, 696 (1932).
  - [3] M.S. Sarandy and D. Lidar, *Phys. Rev. A* **71**, 012331 (2005); *Phys. Rev. Lett.* **95**, 250503 (2005).
  - [4] A.M. Childs, E. Farhi, and J. Preskill, *Phys. Rev. A* **65**, 012322 (2001).
  - [5] J. Roland and N.J. Cerf, *Phys. Rev. A* **71**, 032330 (2005).
  - [6] M. Tiersch and R. Schützhold, *Phys. Rev. A* **75**, 062313 (2007).
  - [7] M.H.S. Amin, P.J. Love, and C.J.S. Truncik, *Phys. Rev. Lett.* **100**, 060503 (2008).
  - [8] A.T.S. Wan, M.H.S. Amin, and S. Wang, *cond-mat/0703085*.
  - [9] M.H.S. Amin and D.V. Averin, *arXiv:0708.0384*.
  - [10] K. Blum, “Density Matrix Theory and Applications”, Plenum Pub. Corp., New York, 1st edition (1981).
  - [11] U. Weiss, “Quantum Dissipative Systems”, World Scientific, Singapore, 2nd edition (1999).
  - [12] A.J. Leggett *et al.*, *Rev. Mod. Phys.* **59**, 1 (1987).
  - [13] D.A. Meyer and N.R. Wallach, *J. Math. Phys.* **43**, 4273 (2002).
  - [14] W.K. Wootters, *Phys. Rev. Lett.* **80**, 2245 (1998).
  - [15] As was shown in [7], a superohmic environment may change the scaling of the computation.